Paper 041

SHAFT ANGLE CORRECTIONS FOR ROTOR TESTS IN A CLOSED SECTION WIND TUNNEL

M. Boffadossi, M. Valentini, L. Vigevano

Dipartimento di Scienze e Tecnologie Aerospaziali - Politecnico di Milano, Via La Masa 34, 20156 Milano, Italy

Abstract

The present work applies a recently developed method[1] to compute, by means of coupled CFD/CSD simulations, the shaft angle corrections for closed section wind tunnel tests on trimmed isolated rotor configurations. A complete simulation of the rotor flow field in free-flight is performed, and the power coefficient C_P is extracted. Then a set of simulations of the same rotor at the same trim state is performed in the closed section of Politecnico di Milano large wind tunnel at different shaft angles. The power coefficient is extracted from each simulation in order to evaluate the shaft angle which matches the C_P value obtained in free-flight. The computations are performed using a trimmed actuator disc model with non uniform source distribution, coupling the CFD code *ROSITA* with the CSD code *MBDyn*.

The methodology is applied spanning the available tunnel velocity range. Two different rotor trim conditions are evaluated: zero flapping angle trim and shaft moment trim. The achieved corrections for the two trimming options are compared and discussed.

1 Introduction

Model rotor tests carried out in closed test sections, even in large wind tunnels, represent a difficult task, because the wall interference is unavoidable and can be as large as to make completely insignificant the test results themselves. This *flow breakdown* phenomenon occurs when operating the model rotor at low tunnel speed and high thrust conditions. In these conditions the interaction between the rotor wake and the tunnel walls strongly modify the flow in the vicinity of the rotor due to the onset of recirculation[2–7], and the measured rotor performances cannot be thought as representative of the rotor free-flight conditions. A qualitative assessment of the flow breakdown conditions in the closed test section of Politecnico di Milano (PoliMi) large wind tunnel was reported in[7,8].

For tunnel and model rotor operating conditions that avoid flow breakdown, the closed section walls induce eventually a flow upwash, not uniformly distributed over the rotor disk, and the measured torque is lower than the free-flight value. However, in this case quantitative measures to correct for the wall interference effect, analogue to the angle-of-attack corrections for fixed wing tests, may be sought. A rotary wing, Glauert type correction, as proposed in[5], may be written as:

$$\mathit{\Delta}\alpha_{\mathrm{s}} = \alpha_{\mathrm{s,free}} - \alpha_{\mathrm{s,wt}} = \frac{180}{\pi}\frac{2\delta_{\mathrm{wt}} C_{\mathrm{T}} A}{\mu^2 A_{\mathrm{wt}}}, \quad (1)$$

where $\alpha_{\mathrm{s,free}}$ and $\alpha_{\mathrm{s,wt}}$ are the shaft angles in free-flight and wind tunnel tests, respectively, μ the advance ratio, A the rotor disk area, A_{wt} the wind tunnel test section area, C_{T} the rotor thrust coefficient and δ_{wt} a correction coefficient specific to the wind tunnel, which is typically positive for closed test sections. The normalization factor $180/\pi$ that appears in the right hand side of equation (1) is needed to convert $\mathit{\Delta}\alpha_{\mathrm{s}}$ to degrees since δ_{wt} is customarily given in radians.

The correction coefficient δ_{wt} may be obtained from experiments or analytically. Heyson[9–13] proposed a potential flow theory based on a dipole wake modeling, later improved by Brooks *et al.* [14], which expresses the correction in terms of induced velocity variations. A fully CFD approach that compares simulations in free-flight to simulations in open wind tunnel sections was proposed by Biava *et al.*[1].

The objective of the present work is to apply the same CFD approach but in closed wind tunnel sections.

The structure of this paper is as follows. Section 2 briefly describes the computational tools utilized for the rotor tests simulations, the trimmed Actuator Disk (AD) model employed and the shaft angle correction procedure. Section 3 summarizes, with some numerical details, the set of numerical simulations, carried out in the wind tunnel environment and in free flight with the coupled CFD/CSD method. Section 4 reports the achieved results. Some conclusions are drawn in the last section.

2 Computational tools

To reduce the computational cost of the CFD simulations, a trimmed AD model[15] with non uniform source distribution was utilized. The model fully accounts for the blade dynamics. The source distribution and the orientation of the disk with respect to the shaft axis are adapted during the simulation, in order to meet the prescribed trim state. Blade loads are computed with the standard Blade Element Theory (BET) with gas velocity provided by the CFD solution, while blade dynamics is represented by a multi-body description of the rotor using the *MBDyn* code[16].

MBDyn is a free general-purpose multi-body analysis software mildly oriented towards the analysis of rotorcraft systems through the availability of simplified built-in rotor blade aerodynamics. The analysis is based on the integration in time of the Newton-Euler equations of motion of a set of discrete bodies, subjected to configuration-dependent forces that model deformability and aerodynamic loads, and connected by kinematic constraints expressed using the Lagrangian multipliers formalism[17]. The modularity of the formulation eases the coupling with the CFD solver.

The trimmed AD model has been embedded in *ROSITA*[18,19], a compressible solver developed at Politecnico di Milano. *ROSITA* numerically integrates the RANS equations, coupled with the one-equation turbulence model of Spalart–Allmaras[20], in systems of moving, overset, multi-block grids. The use of a system of overset grids (Chimera) allows to give the actuator disc grid the same orientation as the rotor tip path plane without the need of remeshing. The adopted Chimera approach is derived from that originally proposed by Chesshire and Henshaw[21], with modifications to further improve robustness and performance. Within *ROSITA*, the governing equations are discretized in space by means of a cell-centered finite-volume implementation of the Roe's scheme[22]. Second order accuracy is obtained through the use of MUSCL extrapolation supplemented with a modified version of the Van Albada limiter introduced by Venkatakrishnan[23]. The viscous terms are computed by the application of the Gauss theorem and using a cell-centered discretization scheme. Time advancement is carried out with a dual-time formulation[24], employing a 2nd order backward differentiation formula to approximate the time derivative and a fully unfactored implicit scheme in pseudo-time. The generalized conjugate gradient (GCG), in conjunction with a block incomplete lower-upper preconditioner, is used to solve the resulting linear system. To compute the low speed, steady flows considered in the present work, Turkel's[25] low Mach preconditioner has been employed.

The coupled CFD/CSD method proceeds as follows:

(a) *MBDyn* computes an initial trim state using one of its embedded simple inflow models and provides a rotor load map (a radial and azimuthal load distribution) and the disk orientation to *ROSITA*.

(b) *ROSITA* is then run until a steady inflow condition is reached at the disk surface, thus providing an updated inflow map to the CSD solver.

(c) *MBDyn* uses the CFD inflow map to compute a new trimmed solution and to find the updated load distribution on the rotor.

Points (b) and (c) are repeated until the variation of the rotor commands between to successive coupling cycles is below a prescribed tolerance. The coupling method has demonstrated to be able to reach a converged solution within 5-10 cycles. This is illustrated in figures 1 and 2, where the evolution during the iteration cycle of, respectively, the rotor load map and the normalized power coefficient is shown.

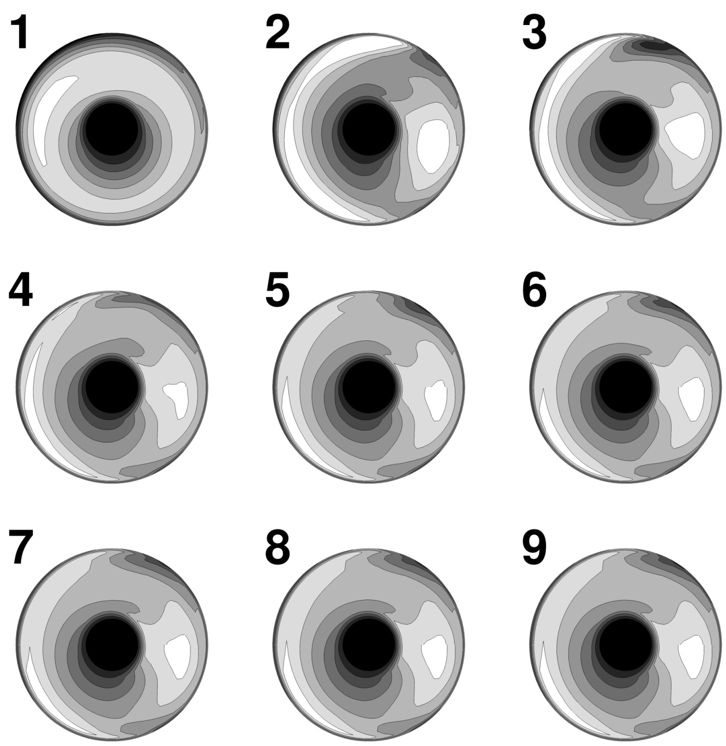

Figure 1: Evolution of the rotor load map during the *ROSITA/MBDyn* iteration cycle

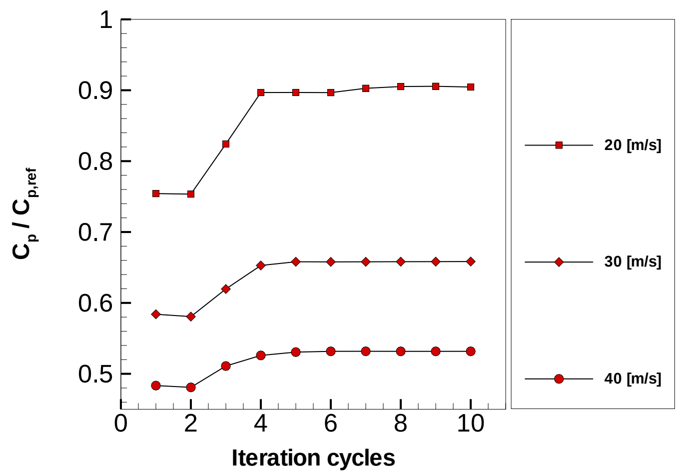

Figure 2: Convergence of the iteration cycle at different speeds. Zero-Flap trim at $C_{\mathrm{T}}/\sigma = 0.1$

The coupled CFD/CSD method has been employed to simulate both the model rotor in the closed test section and a geometrically similar full-scale rotor in free-flight. Keeping constant the trim target in terms of thrust coefficient and flapping angles or mast loads, the rotor performance in terms of power coefficient have been matched by varying the shaft angle in the wind tunnel set up. The comparison between the results relative to the two different environments and geometric scales led to the definition of a shaft angle correction procedure, that permits to correlate the wind tunnel measurements to the performance of the real rotor in free flight.

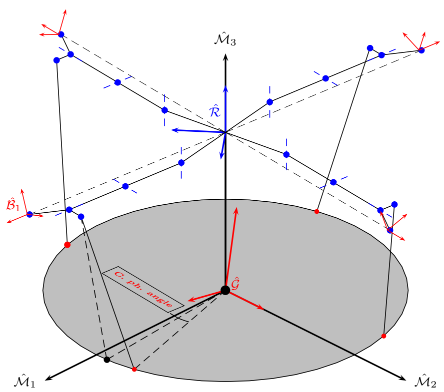

Figure 3: Multi-body model for the rotor mast and blades

For each reference condition in free-air, three simulations have been performed in the wind tunnel, with a step of three degrees on the shaft angle, and then a linear interpolation was performed in the plane $(\alpha_{\text{shaft}}, C_{\text{P}})$.

3 Numerical calculations

The main target of a shaft angle correction is to reproduce in the wind tunnel the same performance the rotor features in free-flight. During the experimental tests on model rotors in the wind tunnel, a choice is made on how to trim the rotor. Usually a zero flapping trim is selected, because it eases the control of the model rotor. This choice of the trim setting has to be accounted for when applying the present CFD methodology for evaluating the shaft angle correction.

In the previous work proposed by Biava *et al.*[1] a zero flap condition is imposed both in wind tunnel and in free air, but other choices are possible. In the present work two different trim condition are considered:

(a) In the first trim option, labelled zero flap-trim, the rotor is forced to have a zero flap condition, both in the wind tunnel and free-flight. The major drawback of this approach is that the zero flap correction in free air is not representative of a real flight condition.

(b) In the second trim procedure, labelled moment-trim, a reasonable flight condition is considered, in terms of C_{T}, tip path plane angles, shaft angle, and the moment coefficients on the rotor mast are computed. Then, in the wind tunnel simulation, the rotor is trimmed so as to reproduce the same C_{T} and mast moment coefficients as in free-flight.

The employed *MBDyn* model (figure 3) defines a 4-bladed model rotor, implementing a high fidelity reproduction of the whole rotor kinematics, including the complete articulation mechanism of the hinges and pitch links. The aerodynamic tables for the blade airfoils, to be used in the BET discretization (figure 4) of the trimmed AD model, were computed for an average value of the Re/M (Reynolds over Mach) of 2×10^6, for the model-scale rotor.

Figure 5 shows the numerical domain used for the free-flight simulations. The Chimera grid system consists of three components: a background mesh which extends up to the far-field; a transition grid, with intermediate density, to better capture the rotor wake; a cylindrical mesh for the actuator disk. The resulting mesh contains about 2.5 million cells.

Figure 6 shows the numerical domain used for the simulations in the wind tunnel. The Chimera grid system consists in this case of only two components: a background mesh which represents the wind tunnel chamber and a cylindrical mesh for the actuator disk. The resulting mesh contains about 1.5 million cells.

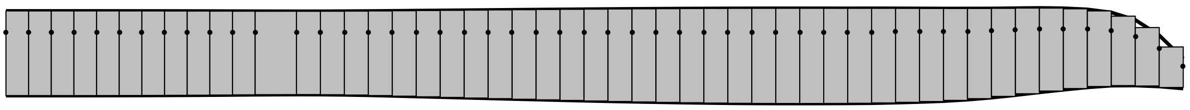

Figure 4: Blade Element Theory discretization

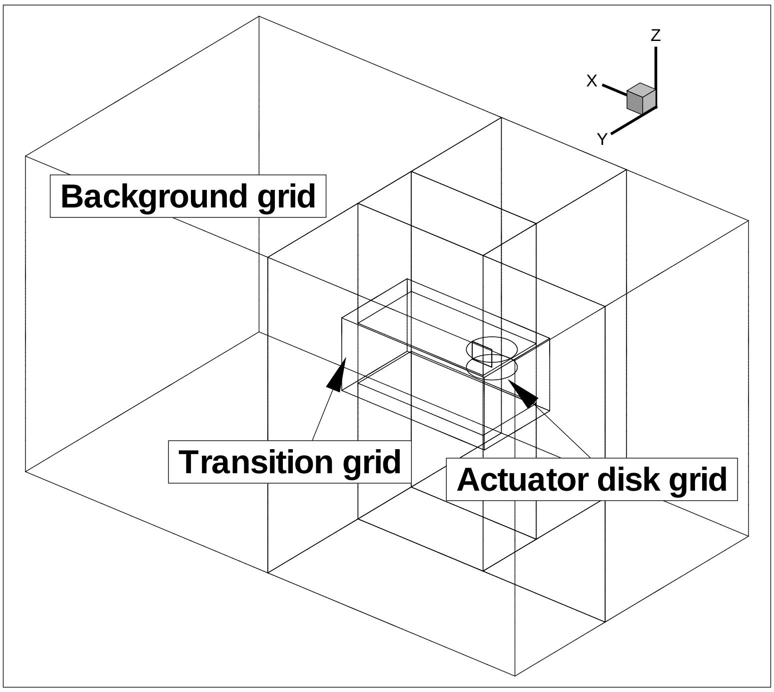

Figure 5: Free-flight flow domain and grid layout

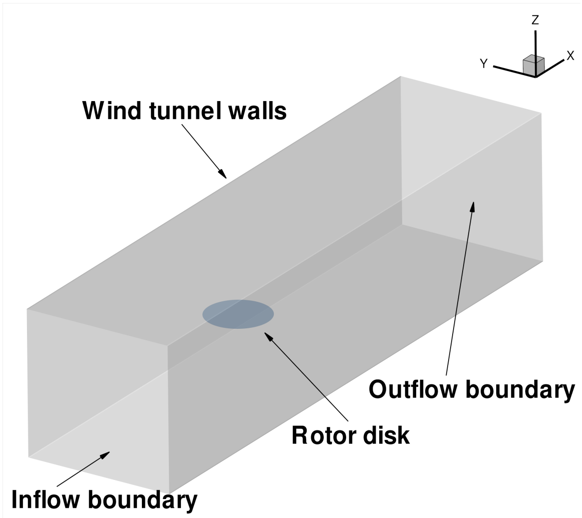

Figure 6: Closed test section flow domain

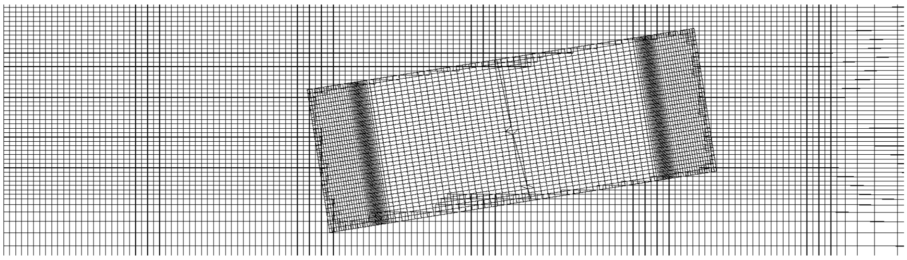

Figure 7: Grid section in the closed test section

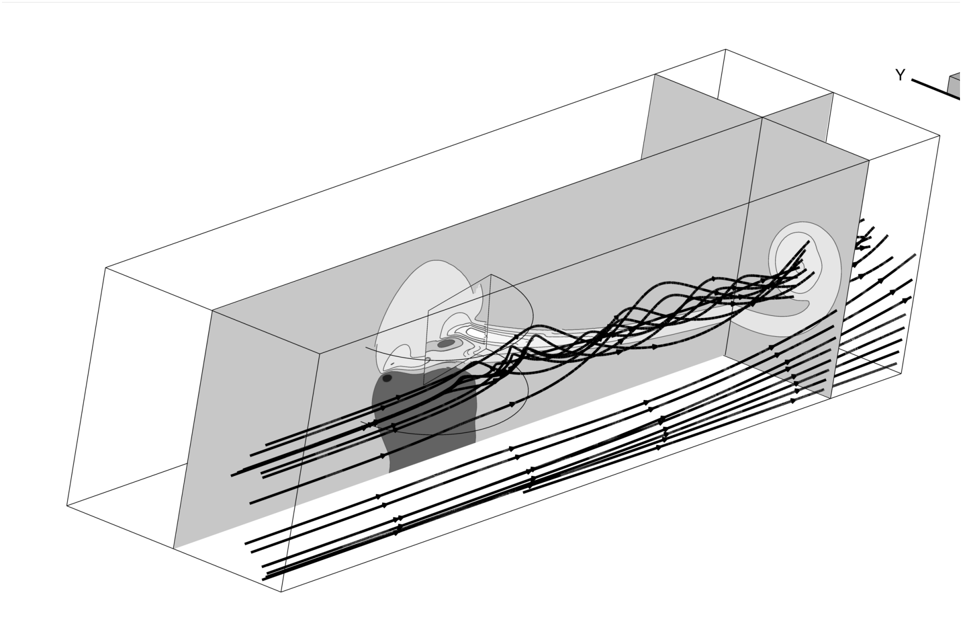

Figure 8: Flow field visualization of the rotor in the wind tunnel. $V = 20m/s, C_{\mathrm{T}}/\sigma = 0.1$

Trim option	β_{1S} $[^o deg.]$	β_{1C} $[^o deg.]$	Speed range [m/s]	C_{T}/σ range
zero flap	0.0	0.0	20-40	0.08-0.1
mast moments	3.1	2.6	20-40	0.1

Table 1: Trim options and operating conditions

Figure 7 shows a slice of the computational mesh in the symmetry plane of the wind tunnel, where the two component grids can be clearly viewed. An example of the computed flow field at the lower end of the tunnel velocity range is given in fig. 8, in which it is clearly visible the vortex generated by the rotor disk into the wind tunnel.

The trim configurations and the operating range covered by the simulations are reported in Table 1.

For all the presented simulations the *ROSITA* solver was run in parallel on 8 processors for the closed section and 32 processors for the free air. The simulations took 5 to 10 *ROSITA/MBDyn* coupling cycles to converge, depending on the operating conditions, but it generally takes longer for low wind speeds. At each coupling cycle *ROSITA* was run performing 2000 pseudo-time iterations at CFL=5.0; the cycle computational time was 5 hours (wall clock). The time consumed by *MBDyn* at each cycle is roughly 5 minutes and it is therefore negligible.

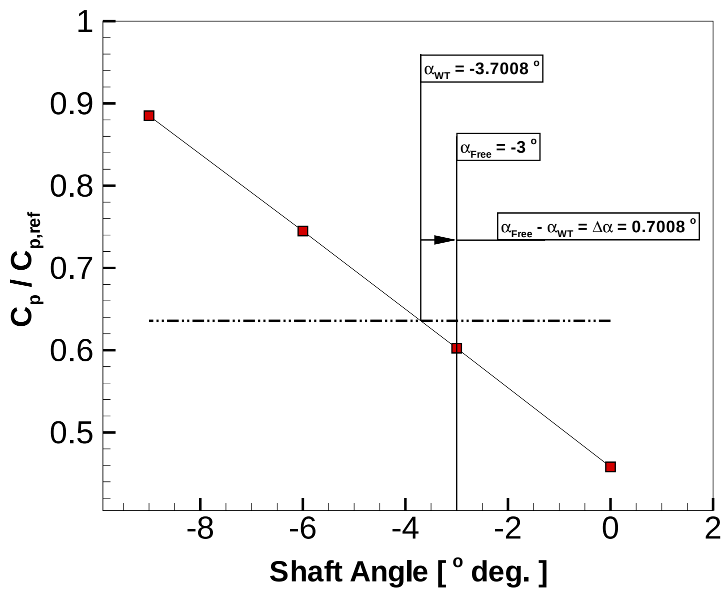

Figure 9: Example of shaft angle correction procedure at $C_\mathrm{T}/\sigma = 0.08$ and V = 40.0 [m/s]

4 Discussion of results

A typical result of the shaft angle correction procedure is illustrated in fig. 9, where the power coefficient for the zero flap-trim calculations in the wind tunnel is reported as function of the shaft angle of the model rotor. The variation of C_P with $\alpha_{\mathrm{s,wt}}$ is linear and the shaft angle correction is immediately obtained matching the free-flight C_P value. It is interesting to note that the correction is always obtained by interpolation, in the whole velocity range considered. Figures 10 and 11 show the free-flight C_P values as function of the free-stream velocity, at a fixed shaft angle, together with the wind tunnel C_P values for different shaft angles. The free-flight curve lies always within the range of the wind tunnel results.

4.1 Zero flap-trim

The achieved results for the zero flap-trim option at the two considered C_T/σ values are summarized in figures 12 and 13, where the shaft angle correction $\Delta\alpha_\mathrm{s}$ and the correction coefficient δ_{wt}, as defined in (1), are shown. In the figures, a comparison is made between the present results and those obtained using Heyson's method[13]. We remark here that Heyson's correction method is influenced only by the geometrical characteristics of the model rotor and tunnel test section, the C_T value and the inclination of the rotor disk with respect to the free stream velocity.

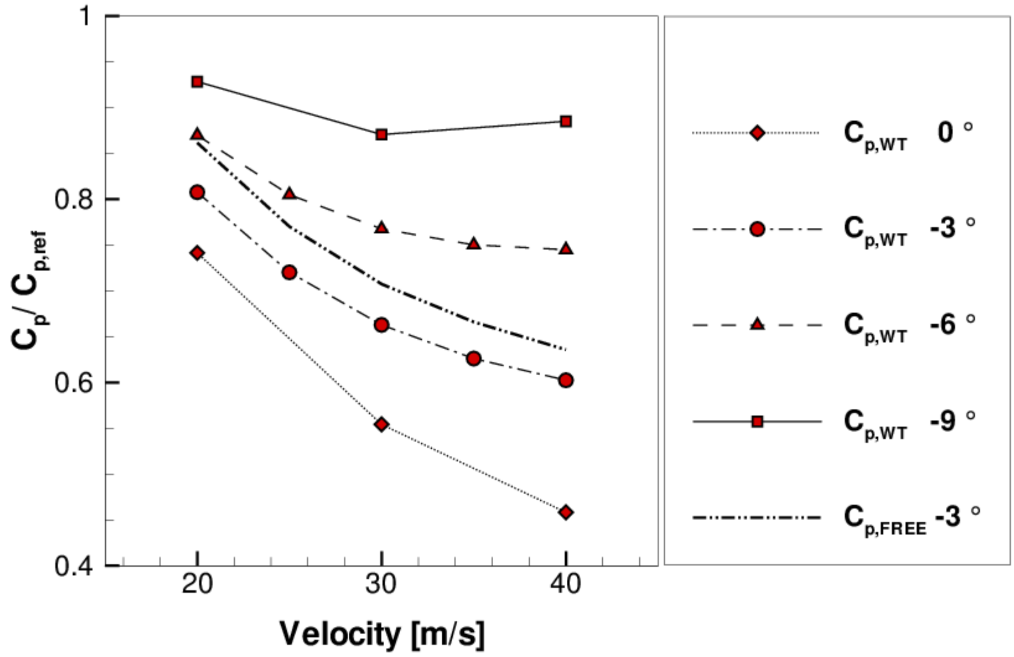

Figure 10: Computed values of the normalized torque coefficient for $C_{\mathrm{T}}/\sigma = 0.08$ and various shaft angles

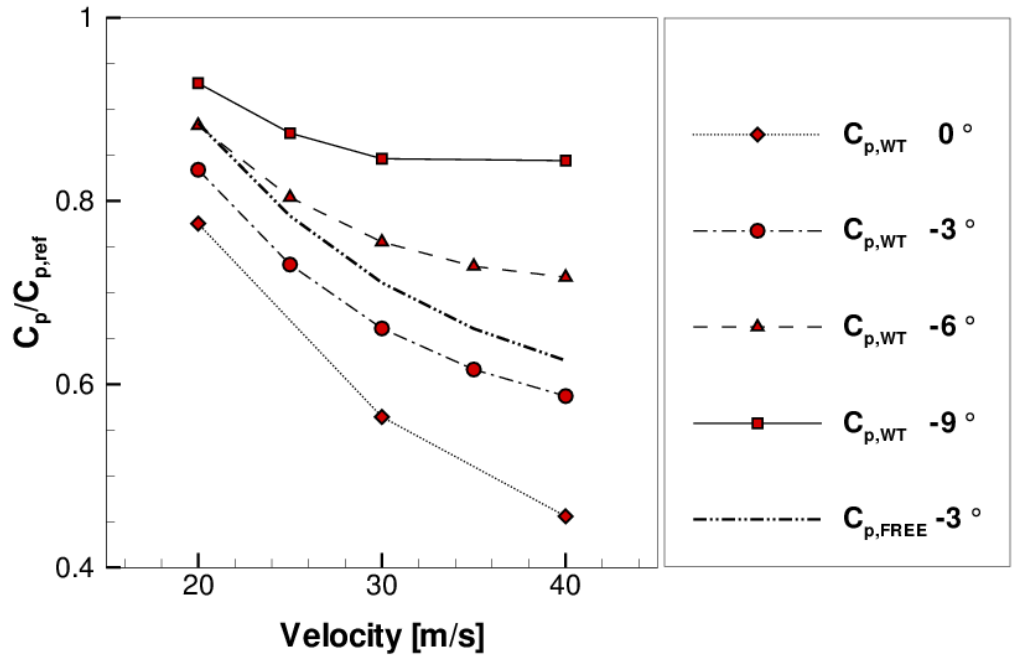

Figure 11: Computed values of the normalized torque coefficient for $C_{\mathrm{T}}/\sigma = 0.1$ and various shaft angles

For the present case, Heyson's method has been applied considering a disk inclination of -3 deg, corresponding to a zero flap-trim at $\alpha_\mathrm{s} = -3$ deg as reference free-flight condition.

The α_s corrections of the present method and Heyson's agree quite noticeably. When we convert the $\Delta\alpha_\mathrm{s}$ into the correction coefficient δ_wt rewriting the Glauert formula (1) as:

$$\frac{V^2}{\mathcal{K}}\,\Delta\alpha_\mathrm{s} = \delta_\mathrm{wt}$$

with:

$$\mathcal{K} \triangleq 2\,C_\mathrm{T} V_\mathrm{TIP}^2\,\frac{180}{\pi}\,\frac{A}{A_\mathrm{wt}}$$

we can notice some differences. However, these differences are magnified by the quadratic dependence of δ_wt from the free stream velocity. In order to better appreciate this, we reported in the right part of figures 12 and 13 two lines obtained varying the Heyson's $\Delta\alpha_\mathrm{s}$ value by 0.1 deg and computing the corresponding δ_wt variations. The present results lay well within these bounds.

We can also observe that the shaft correction expression (1) does not match the present results completely, since the correction coefficient δ_wt is not constant over the complete velocity range.

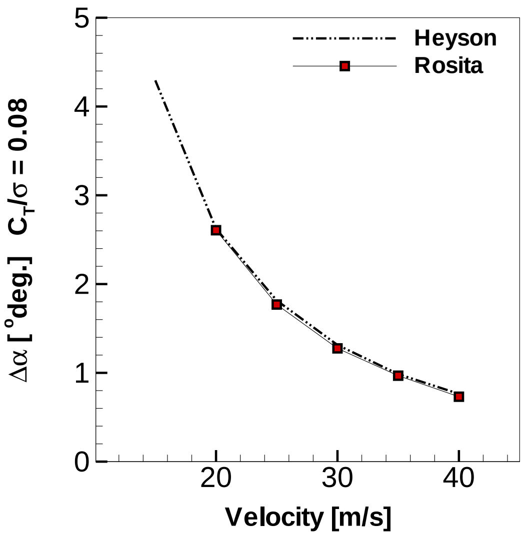

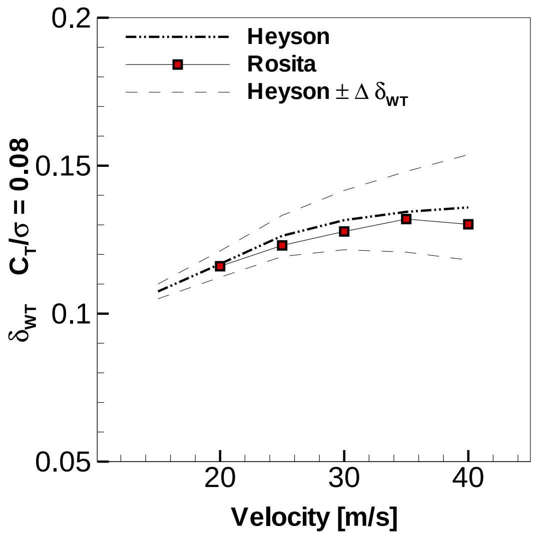

Figure 12: Zero flap-trim shaft angle correction (left) and δ_wt coefficient (right) for $C_\mathrm{T}/\sigma = 0.08$

4.2 Moment-trim

The moment-trim option reference condition in free-flight considers a shaft angle inclination of -3 deg and an assigned first harmonic of the flapping angle with $\beta_{1\mathrm{s}} = 2.6$ deg and $\beta_{1\mathrm{c}} = 3.1$ deg. The model rotor in the wind tunnel is trimmed to the mast moments computed in such reference condition. The differences in the tip path plane angles between free-flight and wind tunnel conditions is on the order of 0.05 deg, in both *sin* and *cos* components.

The results for the moment-trim option are reported in fig. 14. They are compared with Heyson's results with disk inclination of -3 deg, as in the previous section. The shaft angle correction with the moment-trim, predicted by the present method, is therefore slightly lower than that predicted with the zero flap-trim. This difference can be explained considering that a portion of the correction is *absorbed* by the different tip path plane of the rotor, which is free to change orientation in order to satisfy the constraints on the moments.

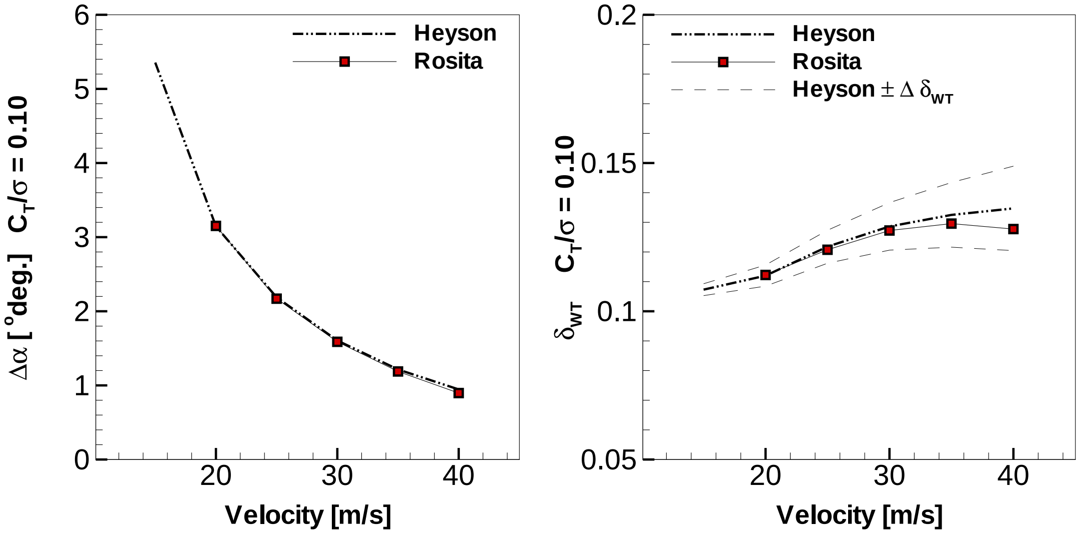

Figure 13: Zero flap-trim shaft angle correction (left) and δ_{wt} coefficient (right) for $C_{\mathrm{T}}/\sigma = 0.10$

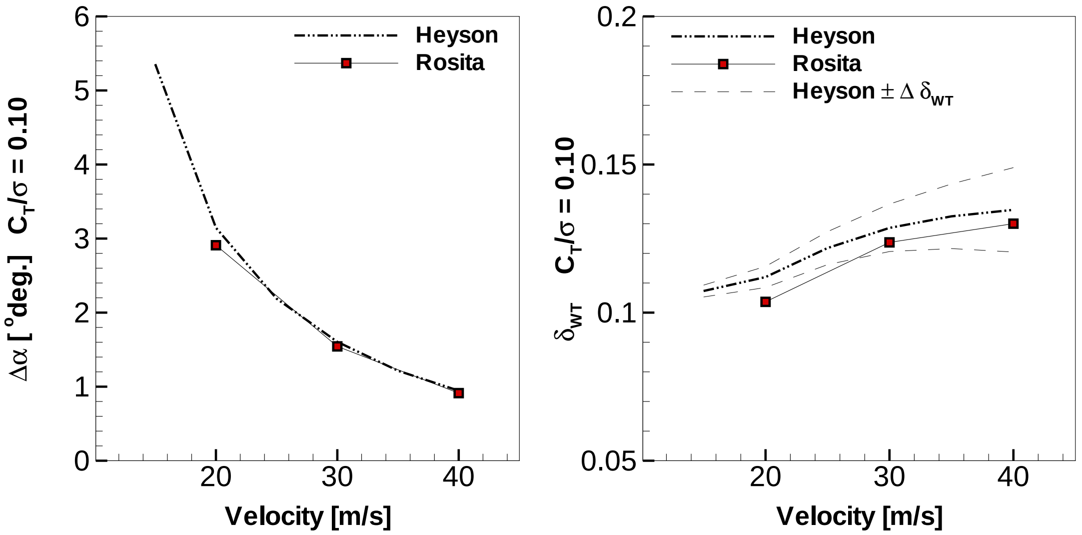

Figure 14: Moment-trim shaft angle correction (left) and δ_{wt} coefficient (right) for $C_{\mathrm{T}}/\sigma = 0.10$

5 Conclusions

The main outcome of the present work is the definition of the shaft angle correction coefficient for the PoliMi large wind tunnel with closed section, so as to predict with accuracy the performance of full-scale rotors in free-flight starting from measurements on model rotors. The obtained result seems to confirm the results obtained by Heyson's analytical method[13].

The effect of the choice of the trim procedure to be employed during the experimental tests is quantitatively not very important, with a smaller correction coefficient computed for the moment-trim option than for the zero flap-trim option.

Acknowledgements: The authors wish to thanks Dr. B. van der Wall, DLR, for kindly providing a correct version of Heyson's code

References

[1] M. Biava, M. Valentini, and L. Vigevano. Wind Tunnel Corrections for Isolated Rotor Tests. In 39^{th} *European Rotorcraft Forum, Moscow, Russia, paper 69*, 2013.

[2] W.H. Rae Jr. Limits on Minimum-Speed V/STOL Wind-Tunnel Tests. *Journal of Aircraft*, 4(3):249–254, 1967.

[3] F.D. Harris. Aerodynamic and Dynamic Rotary Wing Model Testing in Wind Tunnels and Other Facilities. In *AGARD LS 63 "Helicopter Aerodynamics and Dynamics"*, 1973.

[4] J.-J. Philippe. Consideration on wind-tunnel testing techniques for rotorcrafts. In *AGARD Special Course on Aerodynamics of Rotorcraft*, 1990.

[5] H.J. Langer, R.L. Peterson, and T.H. Maier. An Experimental Evaluation of Wind Tunnel Wall Correction Methods for Helicopter Performance. In *American Helicopter Society* 52^{nd} *Annual Forum Proceedings*, 1996. Washington, DC.

[6] P. M. Shinoda. Wall interaction effects for a full-scale helicopter rotor in the NASA Ames 80-by 120-foot wind tunnel. In *AGARD Meeting on "Wall Intereference, Support Interference and Flow Field Measurements"*, 1993.

[7] M. Biava, A. Thomopoulos, and L. Vigevano. Computational assessment of flow breakdown in closed section model rotor tests. In 37^{th} *European Rotorcraft Forum, Vergiate/Gallarate, Italy*, 2011.

[8] M. Biava and L. Vigevano. Computational Assessment of Wind Tunnel Flow in Closed and Open Section Model Rotor Tests. *Journal of the Americal Helicopter Society*, 59, 012006, 2014.

[9] H.H. Heyson. Jet-Boundary Corrections for Lifting Rotors Centered in Rectangular Wind Tunnels. Technical Report TR R-71, NASA, January 1960.

[10] H.H. Heyson. Use of Superposition in Digital Computers to Obtain Wind-Tunnel Interference Factors for Arbitrary Configurations, with Particular Reference to V/STOL Models. Technical Report TR R-302, NASA, February 1969.

[11] H.H. Heyson. Fortran Programs for Calculating Wind-Tunnel Boundary Interference. Technical Report TM X-1740, NASA, February 1969.

[12] H.H. Heyson. Theoretical Study of Conditions Limiting V/STOL Testing in Wind Tunnels with Solid Floor. Technical Report TN D-5819, NASA, June 1970.

[13] H.H. Heyson. Rapid Estimation of Wind Tunnel Corrections with Applications to Wind Tunnel and Model Design. Technical Report TN D-6416, NASA, September 1971.

[14] P. Beaumier, J. Prieur, G. Rahier, P. Spiegel, A. Demargne, C. Tung, J.M. Gallman, Y.H. Yu, R. Kube, B.G. Van der Wall, K.J. Schultz, W.R. Splettstoesser, T.F. Brooks, C.L. Burley, and D.D. Boyd Jr. Effect of Higher Harmonic Control on Helicopter Rotor Blade-Vortex Interaction Noise: Prediction and Initial Validation. In *AGARD Conference Proceedings CP-552 "Aerodynamics and Aeroacoustics of Rotorcraft"*, 1994.

[15] M. Biava, M. Valentini, and L. Vigevano. Trimmed Actuator Disk Modeling for Helicopter Rotor. In 39^{th} *European Rotorcraft Forum, Moscow, Russia, paper 94*, 2013.

[16] Mbdyn - multibody dynamics http://www.aero.polimi.it/mbdyn/.

[17] G. Ghiringhelli, P. Masarati, P. Mantegazza, and M.W. Nixon. Multi-body analysis of a tiltrotor configuration. *Nonlinear Dynamics*, 19:333–357, 1999.

[18] M. Biava. *RANS computations of rotor/fuselage unsteady interactional aerodynamics*. PhD thesis, Dipartimento di Ingegneria Aerospaziale, Politecnico di Milano, 2007.

[19] M. Biava, W. Khier, and L. Vigevano. CFD prediction of air flow past a full helicopter configuration. *Aerospace Science and Technology*, 19:3–18, 2012.

[20] P.R. Spalart and S.R. Allmaras. One equation model for aerodynamic flows. In 30^{th} *AIAA Aerospace Science Meeting & Exhibit, Reno, NV. AIAA 92-0439*, 1992.

[21] G. Chesshire and W. D. Henshaw. Composite overlapping meshes for the solution of partial differential equations. *Journal of Computational Physics*, 90:1–64, 1990.

[22] P.L. Roe. Approximate Riemann Solvers, Parameter Vectors and Difference Schemes. *Journal of Computational Physics*, 43:357–372, 1981.

[23] V. Venkatakrishnan. On the accuracy of limiters and convergence to steady state solutions. In 31^{st} *AIAA Aerospace Sciences Meeting and Exhibit, Reno, NV. AIAA 93-0880*, 1993.

[24] A. Jameson. Time dependent calculations using multigrid with applications to unsteady flows past airfoils and wings. In 10^{th} *AIAA Computational Fluid Dynamics Conference, Honolulu, HI. AIAA 91-1596*, 1991.

[25] E. Turkel, R. Radespiel, and N. Kroll. Assessment of preconditioning methods for multidimensional aerodynamics. *Computers & Fluids*, 6:613–634, 1997.